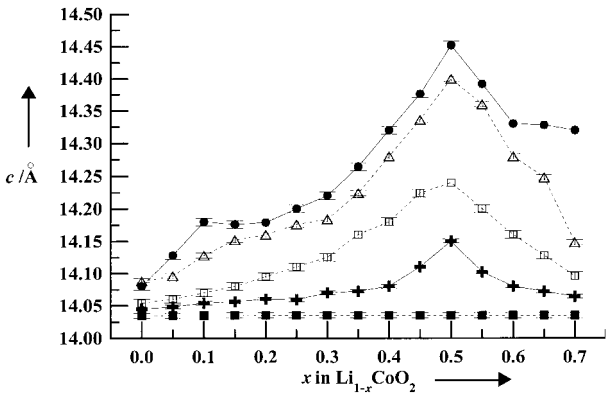

Figure 3. Lattice constants c in ZrO_2 (■), Al_2O_3 (+), TiO_2 (□), B_2O_3 (△) coated, and bare $LiCoO_2$ (●) as a function of x in $Li_{1-x}CoO_2$ during the first charge (c = lattice constant).

nonuniform strain during delithiation produces a new-class of cathode materials, which are extremely tolerant to electrochemical cycling. Note that the lattice constant c of the ZrO_2-coated $LiCoO_2$ exhibits negligible shift in the range $0 < x < 0.7$, which indicates that the original hexagonal symmetry is unaffected by delithiation. A sol–gel coating of ZrO_2, which has the highest fracture toughness, leads to the formation of a fracture-toughened thin-film solid solution (tens of nm thick) near the particle surface. This film significantly improves the structural stability of the cathode material by suppressing c-axis expansion (or phase transition), thereby preventing capacity fading during electrochemical cycling.

In conclusion, the encapsulation of $LiCoO_2$ powders by thin-film coating of high-fracture-toughness oxides effectively suppresses the lattice-constant changes during electrochemical cycling and thereby suppresses phase transitions. The order of capacity retention correlates well with the fracture toughness of the coated thin-film oxides. This innovative technology can be applied to any cathode material that has an accompanying lattice strain (or phase transition) during cycling. The commercial potential of a rechargeable Li-ion battery is enormous.

Experimental Section

Metal (or boron) ethylhexanate-diisopropoxide ($M(OOC_8H_{15})(OC_3H_7)_2$) was dissolved in 2-propanol, and stirred continuously for 20 h at 21 °C. The $LiCoO_2$ powder was then mixed with the coating solution, and the resulting solution was further aged at 50 °C for 24 h to give strong bonds between the metal-oxide (or boron-oxide) gel and the $LiCoO_2$ particle surface. After drying, each coated $LiCoO_2$ powder was fired at 400 °C for 10 h.

To test the cycle-life performance of each cathode material, a slurry of the desired viscosity was prepared by mixing the cathode materials, super P carbon black, and a poly(vinylidene fluoride) (PVDF) binder in a weight ratio of 92:4:4 in *N*-methyl-2-pyrrolidene (NMP; water content was below 0.01 wt%). The coin-type half cell (2016-size) contained a test cathode, a lithium metal counter-and-reference electrode, a 15 μm thick microporous polyethylene separator, and an electrolyte solution of 1M $LiPF_6$ in EC/DMC (1:1 vol% EC = ethylene carbonate, DMC = dimethyl carbonate). Each cell was aged for 24 h at room temperature prior to commencing the electrochemical tests at 21 °C. The coin-type half cells in $Li/LiCoO_2$ were charged with 0.1 C rate to the pre-determined voltages, then potentiostated for 10 h until the current density was equivalent to 0.01 C.

Received: April 17, 2001 [Z16945]

[1] Y.-I. Jang, B. Huang, H. Wang, D. R. Sadoway, G. Ceder, Y.-M. Chiang, H. Liu, H. Tamura, *J. Electrochem. Soc.* **1999**, *146*, 862–868.
[2] H. Wang, Y.-I. Jang, B. Huang, D. R. Sadoway, Y.-M. Chiang, *J. Electrochem. Soc.* **1999**, *146*, 473–480.
[3] K. Dokko, M. Nishizawa, S. Horikoshi, T. Itoh, M. Mohamedi, I. Uchida, *Electrochem. Solid State Lett.* **2000**, *3*, 125–127.
[4] J. Cho, Y. J. Kim, B. Park, *Chem. Mater.* **2000**, *12*, 3788–3791; J. Cho, Y. J. Kim, T.-J. Kim, B. Park, *Chem. Mater.* **2001**, *13*, 18–20.
[5] T. Ohzuku, A. Ueda, N. Yamamoto, *J. Electrochem. Soc.* **1995**, *142*, 1431–1435.
[6] M. M. Thackeray, *J. Am. Ceram. Soc.* **1999**, *82*, 3347–3354.
[7] M. M. Thackeray, *J. Electrochem. Soc.* **1995**, *142*, 2558–2563.
[8] T. Ohzuku, A. Ueda, *J. Electrochem. Soc.* **1994**, *141*, 2972–2977.
[9] G. G. Amatucci, J. M. Tarascon, L. C. Klein, *Solid State Ionics* **1996**, *83*, 167–173.
[10] G. Ceder, Y.-M. Chiang, D. R. Sadoway, M. K. Aydinol, Y.-I. Jang, B. Huang, *Nature* **1998**, *392*, 694–696.
[11] H. Tukamoto, A. R. West, *J. Electrochem. Soc.* **1997**, *144*, 3164–3168.
[12] W. D. Callister, Jr., *Materials Science and Engineering: An Introduction*, Wiley, New York, **1997**, p. 787.
[13] M. C. Fredel, A. R. Boccaccini, *J. Mater. Sci.* **1996**, *31*, 4375–4380.
[14] J. Sehgal, S. Ito, *J. Non-Cryst. Solids* **1999**, *253*, 126–132.

Aromatic Mercury Clusters in Ancient Amalgams**

Aleksey E. Kuznetsov, John D. Corbett,*
Lai-Sheng Wang,* and Alexander I. Boldyrev*

Mercury and its alloys, named amalgams, were known to the Ancients. Amalgams were used for metal extraction from about 500 BC and one of the most interesting influences of

[*] Prof. Dr. J. D. Corbett
Department of Chemistry and Ames Laboratory
Iowa State University
Ames, IA 50011 (USA)
Fax: (+1) 515-294-5718
E-mail: jdc@ameslab.gov
Prof. Dr. L.-S. Wang
Department of Physics
Washington State University
Richland, WA 99352 (USA)
and
W. R. Wiley Environmental Molecular Sciences Laboratory
Pacific Northwest National Laboratory, MS K8-88
P. O. Box 999, Richland, WA 99352 (USA)
Fax: (+1) 509-376-6066
E-mail: ls.wang@pnl.gov
Prof. Dr. A. I. Boldyrev, A. E. Kuznetsov
Department of Chemistry and Biochemistry
Utah State University
Logan, UT 84322 (USA)
Fax: (+1) 435-797-3390
E-mail: Boldyrev@cc.usu.edu

[**] Work done at Utah State University is supported by the donors to The Petroleum Research Fund, administered by the American Chemical Society. Work done at Iowa State University is supported by Basic Energy Sciences, the U.S. Department of Energy. Work done at Washington State University is supported by the National Science Foundation (DMR-0095828) and performed at the W. R. Wiley Environmental Molecular Sciences Laboratory, a national scientific user facility sponsored by DOE's Office of Biological and Environmental Research and located at Pacific Northwest National Laboratory, which is operated for DOE by Battelle.

amalgams (many of which have a golden appearance) on human history was the idea of transmutation (the conversion of base metal into gold). Efforts of transmutation flourished during the time of alchemy, when many gullible rulers of that time found themselves in embarrassing circumstances thanks to the golden appearance of the amalgams. A wide range of alkali metal amalgams is now known with different stoichiometries and structures.[1] Low mercury-content amalgams contain isolated Hg atoms or clusters solvated by the alkali atoms, whereas high mercury-content amalgams tend to have network structures with the alkali atoms occupying interstitial positions. A substantial amount of charge transfer is believed to occur from the alkali metal atoms to mercury in the amalgams. One may think that amalgams, having such a rich and long history, should be well understood today. However, as we will show herein, that is not the case, and the chemistry, structure, and bonding of the amalgams are still not completely elucidated.

What we want to address here is a class of amalgams that contain Hg_4^{6-} square units as their building blocks, typified by that found in solid Na_3Hg_2 (Figure 1).[1, 2] Why Hg_4^{6-} is a particularly stable building block for the amalgams and why it assumes a perfect square structure are questions that have not been understood. To the best of our knowledge, Corbett was the first to examine these questions using molecular orbital (MO) calculations.[3] More recently the electronic structure of mercury amalgams has been studied by Liao using relativistic density functional calculations.[4] However, the aromatic character of the Hg_4^{6-} square units were not discussed. We have obtained a key insight into these questions through the recent discovery of aromaticity in purely metallic clusters.[5–7] We concluded that the square-planar Hg_4^{6-} ion is directly related to this finding and its structure and stability can in fact be attributed to aromaticity.

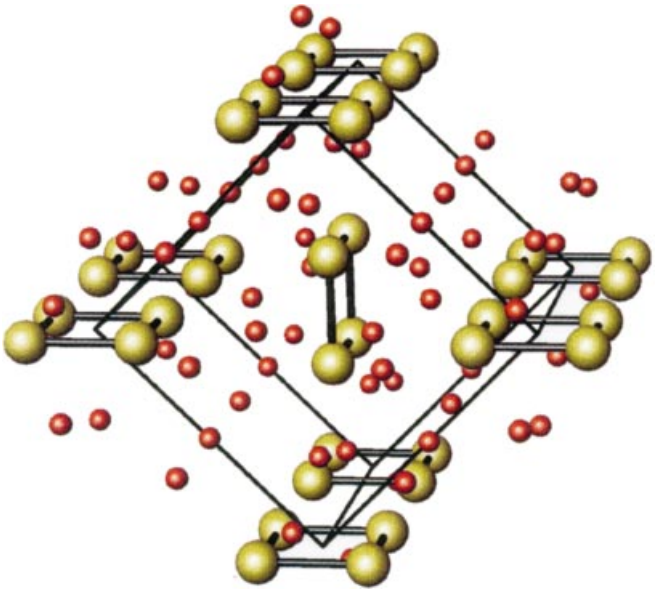

Figure 1. Crystal structure of Na_3Hg_2, showing the Hg_4 square units (yellow) surrounded by Na (red).

We recently reported experimental and theoretical evidence of aromaticity in an all-metal system, the Al_4^{2-} ion in a series of bimetallic and ionic clusters, MAl_4^- (M = Li, Na, or Cu).[5] The Al_4^{2-} ion, both as an isolated species and in the bimetallic clusters, was found to be square-planar and to possess two delocalized π electrons, thus conforming to the structural criterion and the $(4n+2)$ electron-counting rule for aromaticity. A simple electron counting for the Hg_4^{6-} ion immediately revealed that it is isosteric and isoelectronic with the Al_4^{2-} ion if we ignore the d electrons, which can be considered as part of the core. The analogy between Hg_4^{6-} and Al_4^{2-} suggests that the former may be aromatic as well, thus explaining its unique stability and structure.

To confirm this conjecture we performed ab initio calculations on an isolated Hg_4^{6-} ion, as well as on a model neutral Na_6Hg_4 cluster and a known aromatic hydrocarbon analogue $C_4H_4^{2+}$.[8] While the isolated Hg_4^{6-} ion is not expected to be electronically stable as a gaseous species, it is a common practice in chemistry to divide a crystal into building blocks including highly charged anions.[9] For example, *nido*-Tl_4^{8-} is accepted as a building block in Na_2Tl.[10] These charges are only formal charges and do not represent the real electron transfers in the crystals. But they are very important for the proper electron counting in chemistry and for understanding the structure and bonding of the solid building blocks. To test the effects of the counterions on the MOs and bonding on the Hg_4^{6-} building block in the Na_3Hg_2 crystal, while keeping the same electron count, we further performed calculations on a model Na_6Hg_4 cluster. In our calculations for Na_6Hg_4 we used three theoretical methods: a hybrid of Hartree–Fock and density functional methods (B3LYP), a second-order Møller–Plesset perturbation method (MP2), and a complete active space multiconfigurational self-consistent field (CASSCF) calculation, including 103 740 electronic configurations.[11] In all calculations we used the triple-zeta valence basis sets and Stevens–Basch–Krauss effective core potentials (CEP-121G).

Since the purpose of the Na_6Hg_4 calculations was not to determine its global minimum structure, but rather to examine how the presence of Na^+ ions would influence the MOs and bonding in Hg_4^{6-}, it was important to ensure that the Hg_4 unit in the Na_6Hg_4 model has the same symmetry as in the naked Hg_4^{6-}. Our geometry optimization with the D_{4h} symmetry restriction led to the square Hg_4 unit with $R(\mathrm{Hg{-}Hg}) = 2.9-3.1$ Å, depending on the methods used. This calculated Hg–Hg bond length in the model Na_6Hg_4 cluster is actually very close to the value of 3.0 Å for the square Hg_4 cluster observed in the Na_3Hg_2 crystal.[2] This bond length is also very close to the optimized Hg–Hg bond (2.9–3.1) in a linear Na-Hg-Hg-Na molecule. The covalent Hg–Hg bonding in the Na_2Hg_2 molecule is undoubted and therefore the current result lends credence to the Hg–Hg covalent bonding in the model Na_6Hg_4 cluster and the Na_3Hg_2 crystal.

To examine the occupation of MOs we further performed CASSCF calculations on both Hg_4^{6-} and Na_6Hg_4. These calculations show that the Hartree–Fock wave function is predominate in the CASSCF expansion ($C_{HF} = 0.892$), and the occupation numbers for the highest three Hartree–Fock orbitals are close to two, 1.84 e ($2a_{1g}$), 1.87 e ($1b_{2g}$), and 1.85 e

  0044-8249/01/11318-3474 $ 17.50+.50/0

($1a_{2u}$). These results indicate that our one-electron MO picture can be used to understand the bonding of the Hg_4^{6-} cluster in the Na_3Hg_2 amalgams. There is considerable charge transfer from Na to Hg and the model Na_6Hg_4 cluster can be viewed formally as a Hg_4^{6-} cluster solvated by six Na^+ ions. Figure 2a displays the seven valence MOs of the square-planar Hg_4^{6-} and Figure 2b displays those of the Na_6Hg_4 model system. Comparing Figure 2b to 2a, we see clearly that the same set of occupied MOs is present in both cases. The counterions appear to have little effect on the occupied MOs of the Hg_4^{6-} building block; they alter slightly the MO ordering. The MOs shown in Figure 2a are identical to those of Al_4^{2-}, except for the slight difference in ordering among the top three MOs, which are bonding combinations of the valence p orbitals. The bottom four MOs are combinations of the valence s orbitals, which are essentially lone pairs in both Hg_4^{6-} and Al_4^{2-} with little s–p mixing. Based on the presence of the same two π electrons and its square-planar structure, we concluded that Hg_4^{6-} is indeed an aromatic all-metal cluster. To further confirm the aromatic nature of Hg_4^{6-}, we compare its MOs and bonding to those of an aromatic hydrocarbon $C_4H_4^{2+}$, as shown in Figure 2c. $C_4H_4^{2+}$ has four more valence electrons than Hg_4^{6-}. We observed that except for the degenerate HOMO-1 in $C_4H_4^{2+}$, the remaining seven valence MOs of $C_4H_4^{2+}$ are nearly identical to those of Hg_4^{6-}, with its characteristic aromatic π HOMO.

Mercury has a closed shell electron configuration ($6s^2$) and neutral Hg_4 is a van der Waals cluster (the bottom four MOs of Figure 2a or 2b provide no net bonding). The top three MOs of Hg_4^{6-} are completely bonding orbitals formed by perpendicular in-plane p_σ orbitals ($1b_{2g}$), out-of-plane p_π orbitals ($1a_{2u}$), and radial p_σ orbitals ($2a_{1g}$), which are filled owing to electron donation from the alkali metals. On the other hand, the eight σ MOs in $C_4H_4^{2+}$ actually describe four C–C bonds and four C–H bonds, consistent with the classical bonding picture for this saturated hydrocarbon molecule. Compared to $C_4H_4^{2+}$, the aromatic Hg_4^{6-} and Al_4^{2-} species are electron-deficient systems because we do not have four σ MOs to describe four two-electron two-center metal–metal bonds, as the square structure would suggest. Instead, in Hg_4^{6-} and Al_4^{2-}, we only have two four-center σ MOs describing the metal–metal bonding, in addition to the π MO. These multicenter σ bonds have been called σ aromaticity.[12] Hence, the structural and electronic stability of the square-planar Hg_4^{6-} and Al_4^{2-} should be attributed not only to π aromaticity due to the presence of the two π electrons in the $1a_{2u}$ orbital, but also to σ aromaticity due to the occupation of the two four-center σ-bonding orbitals, $1b_{2g}$ and $2a_{1g}$.

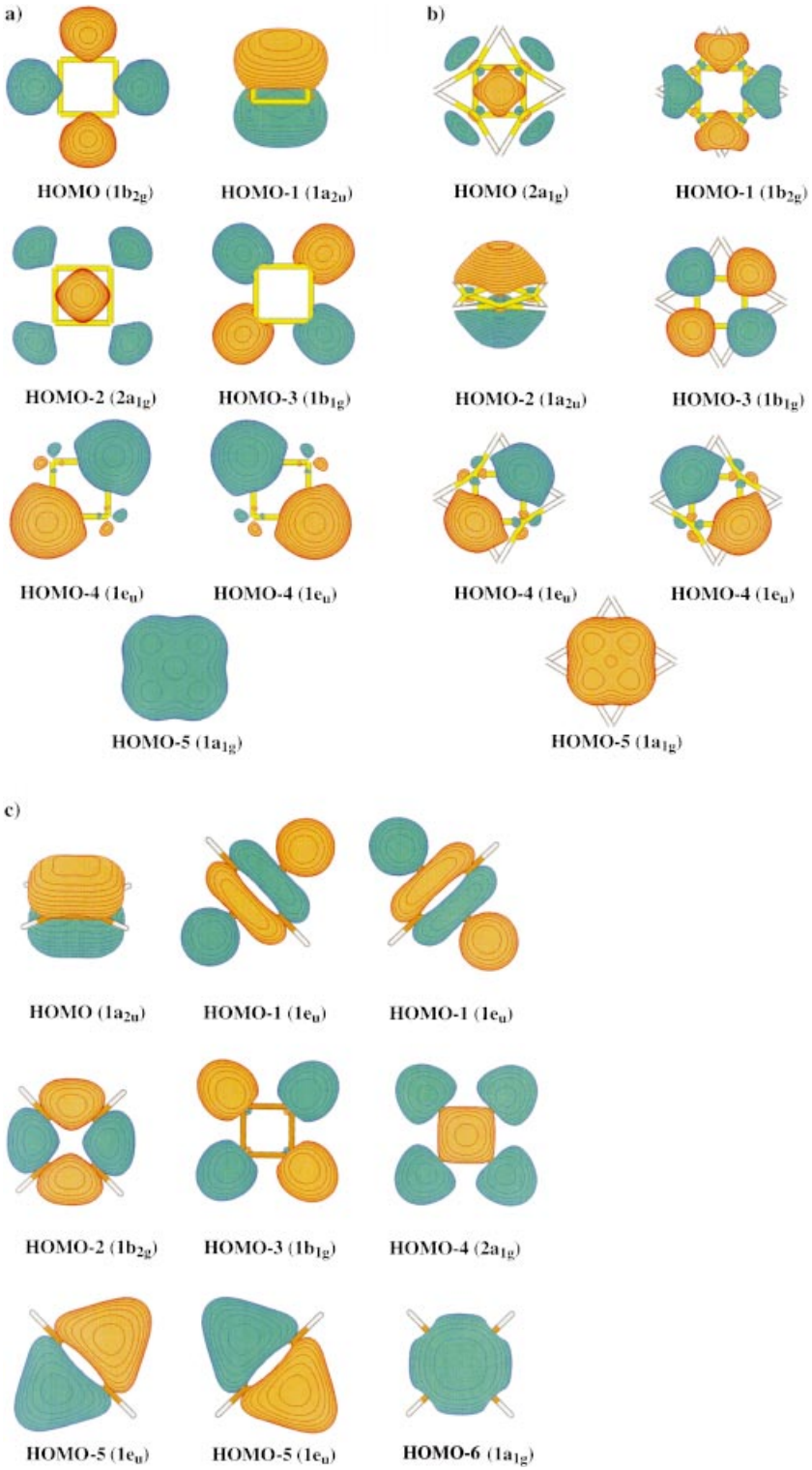

Figure 2. a) Molecular orbital pictures of square-planar Hg_4^{6-}, showing the highest occupied molecular orbital (HOMO, $1b_{2g}$) and the aromatic π orbital (HOMO-1, $1a_{2u}$) down to the fifth valence molecular orbital from the HOMO (HOMO-5, $1a_{1g}$). Note that (HOMO-4) consists of a degenerate pair ($1e_u$). b) Molecular orbital pictures of a model system, Na_6Hg_4, containing a square-planar Hg_4^{6-}. Note the similarity between the MOs in the two systems. c) Occupied molecular orbitals of the aromatic hydrocarbon, $C_4H_4^{2+}$.

Although an analogous aromatic Ga_4^{2-} structural unit has been recently suggested by us to exist in an organometallic

compound,[7] bulk solid materials containing the aromatic Al_4^{2-} ion have not been synthesized. Nevertheless, the current finding of aromaticity in the isoelectronic Hg_4^{6-} ion establishes a solid bridge between our gas-phase studies of aromatic clusters and bulk materials containing such species. It is a pleasant surprise that new insight can still be obtained into such an ancient and well-known material as the amalgam. It is possible that further development in the concept of aromaticity in metallic systems, through gas-phase clusters and model investigations, will lead to discovery of new classes of materials or new insights into the electronic structures and chemical bonding of complex materials.[13]

Received: April 27, 2001
Revised: June 18, 2001 [Z17004]

[1] H. J. Deiseroth, *Prog. Solid State Chem*. **1997**, *25*, 73.
[2] J. W. Nielsen, N. C. Baenziger, *Acta Crystallogr*. **1954**, *7*, 277.
[3] J. D. Corbett, *Inorg. Nucl. Chem. Lett*. **1969**, *5*, 81.
[4] "Relativistic Density Functional Calculations on Heavy Metal Solid Compounds": M. S. Liao, Ph.D. Thesis, University of Siegen, Shaker, Aachen, **1993**.
[5] X. Li, A. E. Kuznetsov, H. F. Zhang, A. I. Boldyrev, L. S. Wang, *Science* **2001**, *291*, 859.
[6] X. Li, H. F. Zhang, L. S. Wang, A. E. Kuznetsov, N. A. Cannon, A. I. Boldyrev, *Angew. Chem*. **2001**, *113*, 1919; *Angew. Chem. Int. Ed*. **2001**, *40*, 1867.
[7] A. E. Kuznetsov, A. I. Boldyrev, X. Li, L. S. Wang, *J. Am. Chem. Soc*. **2001**, in press.
[8] M. Balci, M. L. McKee, P. von R. Schleyer, *J. Phys. Chem. A* **2000**, *104*, 1246.
[9] J. D. Corbett, *Angew. Chem.* **2000**, *112*, 682; *Angew. Chem. Int. Ed*. **2000**, *39*, 670.
[10] F. Smith, D. A. Hansen, *Acta Crystallogr*. **1967**, *22*, 836.
[11] Gaussian 98 (Revision A.7), M. J. Frisch, G. W. Trucks, H. B. Schlegel, G. E. Scuseria, M. A. Robb, J. R. Cheeseman, V. G. Zakrzewski, J. A. Montgomery, R. E. Stratmann, J. C. Burant, S. Dapprich, J. M. Millam, A. D. Daniels, K. N. Kudin, M. C. Strain, O. Farkas, J. Tomasi, V. Barone, M. Cossi, R. Cammi, B. Mennucci, C. Pomelli, C. Adamo, S. Clifford, J. Ochterski, G. A. Petersson, P. Y. Ayala, Q. Cui, K. Morokuma, D. K. Malick, A. D. Rabuck, K. Raghavachari, J. B. Foresman, J. Cioslowski, J. V. Ortiz, B. B. Stefanov, G. Liu, A. Liashenko, P. Piskorz, I. Komaromi, R. Gomperts, R. L. Martin, D. J. Fox, T. Keith, M. A. Al-Laham, C. Y. Peng, A. Nanayakkara, C. Gonzalez, M. Challacombe, P. M. W. Gill, B. G. Johnson, W. Chen, M. W. Wong, J. L. Andres, M. Head-Gordon, E. S. Replogle, J. A. Pople, Gaussian, Inc., Pittsburgh, PA, **1998**..
[12] V. I. Minkin, M. N. Glukhovtsev, B. Y. Simkin, *Aromaticity and Antiaromaticity,* Wiley, New York, **1994**.
[13] D.-K. Seo, J. D. Corbett, *Science* **2001**, *291*, 841.

Allosteric Fluoride Anion Recognition by a Doubly Strapped Porphyrin**

Masayuki Takeuchi, Takeshi Shioya, and Timothy M. Swager*

The design of anion receptors with high selectivity is challenging.[1–6] Most systems developed use complimentary binding sites with hydrogen-bonding groups, quaternary ammonium centers, Lewis acids, and cationic metal ions.[1–6] It is often difficult to control selectivity and sensitivity among anions because of their wide range of geometries, low charge to radii ratios, sensitivities to pH, and high solvation energies.[1a] Receptors for the smallest anion, fluoride, are of special importance for monitoring the fluoride metabolism in nature, the analysis of drinking water,[7] and the detection of chemical warfare agents.[8] We report herein a highly selective allosteric fluoride recognition system[9] by a doubly strapped porphyrin[10] **1** that contains two small hydrogen-bonding cavities that are not able to bind larger anions. It is also demonstrated that a conducting polymer based upon **1** displays both electrochemical and conductivity responses to fluoride ions and no response to chloride ions.

Compound **1** was prepared by condensation of strap moieties **2** with $\alpha\beta\alpha\beta$-tetrakis(2-aminophenyl)porphyrin **3** under high-dilution conditions (Scheme 1).[11, 12] By comparison with related strapped porphyrins containing four linkers, we estimate that the cofacial distance between the phenyls in the straps and the porphyrin is between 3–4 Å.[12] This distance creates a small pocket that is suitable for fluoride-ion binding (the radius of a fluoride anion in an octahedral environment is 1.19 Å[1a, 13]), but should exclude larger anions. The proximate location of the strap moieties to the porphyrin in **1** is confirmed by NMR spectroscopy in $CDCl_3$, which revealed significant upfield shifts of specific signals. The phenyl protons appear at $\delta = 4.24$ which is approximately 2.96 ppm upfield of the dicarboxylate strap precursor. The amide N–H protons resonate at $\delta = 7.68$, which is comparable to closely related phenyl-capped porphyrins which have an additional methylene between the amide carbonyl and the phenyl ether of the strap.[14] These values are very different from unstrapped porphyrins where the same resonances generally appear between $\delta = 5$ and 6.5[10, 15] and suggest that the amide N–H protons are constrained against the porphyrin core. The Soret band of **1** (5.00 μM) in dichloromethane is split into two bands of equal intensity at 404 and 423 nm, which indicate that the strap presents a significant perturbation. This

[*] Prof. T. M. Swager, Dr. M. Takeuchi, Dr. T. Shioya
Department of Chemistry and
Center for Material Science and Engineering
Massachusetts Institute of Technology, Cambridge, MA 02139 (USA)
Fax: (+1) 617-253-7929
E-mail: tswager@mit.edu

[**] This work was funded by the Department of Energy, by a contract through Bechtel Nevada, and the Office of Naval Research. M.T. thanks the Ministry of Education, Science and Culture of Japan for financial support and Prof. Itaru Hamachi and Mr. Masato Ikeda at Kyushu University for helpful discussions.

Supporting information for this article is available on the WWW under http://www.angewandte.com or from the author.

  0044-8249/01/11318-3476 $ 17.50+.50/0